



**ARTICLE**

## Study on the Soy Protein-Based Adhesive Cross-Linked by Glyoxal

Zhigang Wu<sup>1,2,#</sup>, Jiankun Liang<sup>3,#</sup>, Hong Lei<sup>1,\*</sup>, Bengang Zhang<sup>1</sup>, Xuedong Xi<sup>1</sup> and Lifan Li<sup>2</sup>

<sup>1</sup>Yunnan Provincial Key Laboratory of Wood Adhesives and Glued Products, Southwest Forestry University, Kunming, 650224, China

<sup>2</sup>College of Forestry, Guizhou University, Guiyang, 550025, China

<sup>3</sup>Kaili University, Qiandongnan, 556011, China

\*Corresponding Author: Hong Lei. Email: lfxgirl@163.com

#The two authors contributed equally to this work

Received: 15 August 2020 Accepted: 27 October 2020

### ABSTRACT

Based on the ESI-MS and <sup>13</sup>C-NMR analysis of the forms of glyoxal in acidic and alkaline solutions, the soy-based adhesive cross-linked by glyoxal was prepared in this work. The results showed that glyoxal existed in water in different forms at different pH levels. Under alkaline conditions, glyoxal transformed to glycolate through the intramolecular disproportionation reaction. Under acidic conditions, although some of glyoxal transformed to glycolate as what happened under alkaline conditions, most of glyoxal molecules existed in the form of five- or six-membered cyclic ether structure. No ethylene tetraol or free aldehyde group was actually detected under these conditions. Although glyoxal reacted with soy protein under both acidic and alkaline conditions, alkaline conditions were more favorable for the improvement of mechanical performance and water resistance of soy-based adhesives than acid conditions.

### KEYWORDS

Glyoxal; soy protein-based adhesive; cross-link

## 1 Introduction

The development of soy protein-based adhesives has been a hot topic in wood industry today. Some cross-linkers are used to prepare soy-based adhesive with acceptable mechanical performance and water resistance [1–6]. Formaldehyde and its derivatives, such as phenol-formaldehyde resin [7,8], phenol-resorcinol-formaldehyde resin [9], urea-formaldehyde resin [10–12], melamine-formaldehyde [13–15], etc., were proved to be one type of effective cross-linkers of soy-based adhesives. Due to an increasing environmental concern, the addition of toxic formaldehyde has decreased greatly the advantages of soy protein-based adhesives in wood industry. As we all know that formaldehyde was reclassified as a Group 1 “Human Carcinogen” by IARC in 2004.

Compared with formaldehyde, glyoxal is relatively nontoxic and nonvolatile [16,17]. Thus soy protein-based adhesives cross-linked by glyoxal is expected to show better performances on free formaldehyde emission than those cross-linked by formaldehyde. Some work has been reported to substitute part or all of the formaldehyde in urea-formaldehyde resin or melamine-formaldehyde resin with glyoxal [18]. It



was also used as a cross-linker of some bio-based adhesives, such as tannin-based [19,20], lignin-based [21,22] and protein-based adhesives [23,24].

As the simplest dialdehyde, glyoxal has no  $\alpha$ -H structure. It exists in water in different forms and even shows no aldehyde group [25]. The reactions of glyoxal will then be totally different from those of formaldehyde. The pH levels of the glyoxal solution might also affect greatly its existing forms. In this study, on the basis of the analysis of the forms of glyoxal in water under acidic and alkaline conditions, the soy-based adhesive modified by glyoxal was prepared. Although there were some reports on the modification of soy-based adhesive with glyoxal [18,26,27], their emphasis were mostly on the performances of the final resin. The study on the reaction between different forms of glyoxal in water and soy protein was rather few. Although there were some reports on the forms of glyoxal in water [16,17,28–31], there was even actually no undoubted explanation or systematic study on the forms of glyoxal in water at different pH levels. In fact, the pH during the preparation of soy protein-based adhesives has great effects on the performances of the final adhesives [32,33]. In this work, the forms of glyoxal in water at different pH were studied to be a basis for the preparation of soy-based adhesives.

## 2 Materials and Methods

### 2.1 Materials

Soy flour with protein content of 53.4% was from Yuxin Soybean Protein Co., Ltd., China. Glyoxal solution with solid content 40%, NaOH, NaHSO<sub>3</sub> and other chemical reagents in this work were all analytic grade and from Sinopharm Chemical Reagent Co., Ltd., P.R. China. Poplar veneers with a thickness of 1.5 mm and moisture content 8–10% were purchased from Qunyou Wood Co., Ltd., China for the preparation of plywood.

### 2.2 Preparation of Glyoxal Solution Samples at Different pH Levels

The 30% diluted glyoxal was adjusted to pH = 2–3 and pH = 9–10, respectively, with either 10% hydrochloric acid or 10% sodium hydroxide solution. Then these glyoxal solutions were charged to different flasks with magnetic stirrer bars separately and kept at 75–80°C for 1 h under the designed pH levels.

### 2.3 Electrospray Ionization Mass Spectrometry (ESI-MS) Analysis

The glyoxal solution samples at different pH levels were dissolved in chloroform to get a solution with a concentration of 10  $\mu$ L/mL (10  $\mu$ L sample and 1 mL chloroform). The solution was then injected into the ion trap mass spectrometer with ESI via a syringe at a flow rate of 5  $\mu$ g/s. Spectra were recorded in positive mode with ion energy of 0.3 eV on a Waters Xevo TQ-S instrument and the scan range was 0–1000 Da.

### 2.4 <sup>13</sup>C-NMR Analysis

The glyoxal solution samples at different pH levels for <sup>13</sup>C-NMR analysis were prepared by mixing 300  $\mu$ L glyoxal liquid solution sample with 100  $\mu$ L dimethyl sulfoxide-d<sub>6</sub> (DMSO-d<sub>6</sub>). Liquid <sup>13</sup>C-NMR (zgig) spectra were generated using a Bruker Avance spectrometer with a frequency of 600 MHz. To achieve a sufficient signal-to-noise ratio, inverse-gated proton decoupling method was applied. The spectra were obtained at 39062.5 Hz for a number of transients of 800–1200. All the analyses were run with a relaxation delay of 6 s and the chemical shifts were accurate to 1 ppm.

### 2.5 Preparation of Soy Protein-Based Adhesives Modified by Glyoxal Solution

Eighty parts of defatted soy flour, 300 parts of water and 1.6 parts of NaHSO<sub>3</sub> were sequentially charged into a flask equipped with a condenser, thermometer and a magnetic stirrer bar. The mixture was kept at 50°C for 1h to get a soy-based adhesive sample. Then 9.6 parts of glyoxal solution were added to the flask. After

this, the mixture was divided into four parts and the pH of each part were adjusted to 1, 3, 11 and 13, respectively. Corresponded samples with the name of SPG1, SPG3, SPG11 and SPG13 were obtained.

## 2.6 Preparation of Plywood Samples with Soy Protein-Based Adhesive and the Test of Their Shear Strengths

Four soy protein-based adhesives modified with glyoxal solution, that is, SPG1, SPG3, SPG11 and SPG13, were used for the preparation of three-layer plywood samples with the dimensions of 400 mm × 400 mm × 4 mm. Soy protein-based adhesives were applied to both sides of core veneers with a resin loading rate of 300 g/m<sup>2</sup>. Two surface veneers without adhesives were added to both sides of the core veneers. The three-layer plywood assemblies were left at room temperature for 15–20 min before loaded into a XLB type single-opening hot press. The plywood assemblies were pressed under 1.5 MPa at 160°C for 3.5 min.

Before being cut into shear strength specimens of dimensions of 100 mm × 25 mm, plywood samples were conditioned at the chamber of 20 ± 2°C with relative humidity of 65 ± 5% in the laboratory for 1 day. The bonded area of each specimen was 25 mm × 25 mm (Fig. 1). A WDS-50KN mechanical testing machine was used to test the dry and wet shear strength of the plywood specimens respectively following the Chinese national standard GB/T 9846.3-2004 and GB/T 17657-1999. The mean result of 8–10 specimens was used as the final dry or wet shear strength respectively. For wet shear strength, the specimens were soaked in (63 ± 1)°C water for 60 min and then in water under room temperature for 10 min, in accordance with Chinese standards.

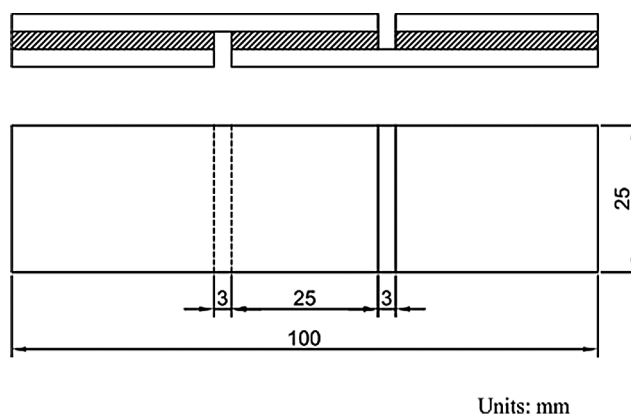


**Figure 1:** The diagram of the plywood

## 3 Results and Discussion

### 3.1 ESI-MS Analysis of Glyoxal Solution

The ESI-MS spectra of glyoxal solution prepared at pH = 9–10 and pH = 2–3 are given in Figs. 2 and 3 respectively. According to the mechanism of ESI-MS, the ion peaks observed in the ESI-MS spectra mainly came from ions  $M + Na^+$ , combination of oxygen atom from glyoxal molecule with  $Na^+$  [24]. (Here, M means molecule.) On the basis of the structure of glyoxal and previous reports [16,17,28–31], Tabs. 1 and 2 summarize the ESI-MS assignments of the main ion peaks of the glyoxal solution samples prepared at pH = 9–10 and pH = 2–3 from Figs. 2 and 3. As is well-known that the isomers with the same molecular weight are possible, Tabs. 1 and 2 give only the most possible structures with relatively low molecular weight.

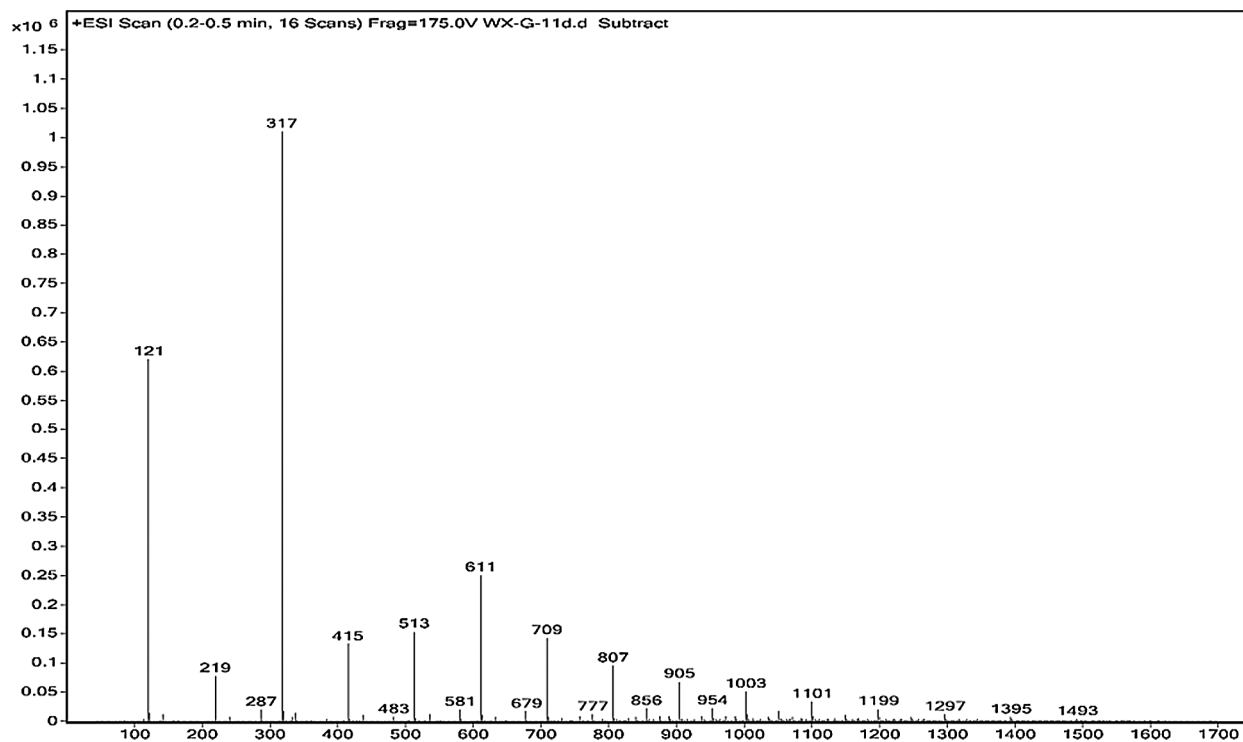


Figure 2: ESI-MS spectrum of glyoxal in alkaline solution

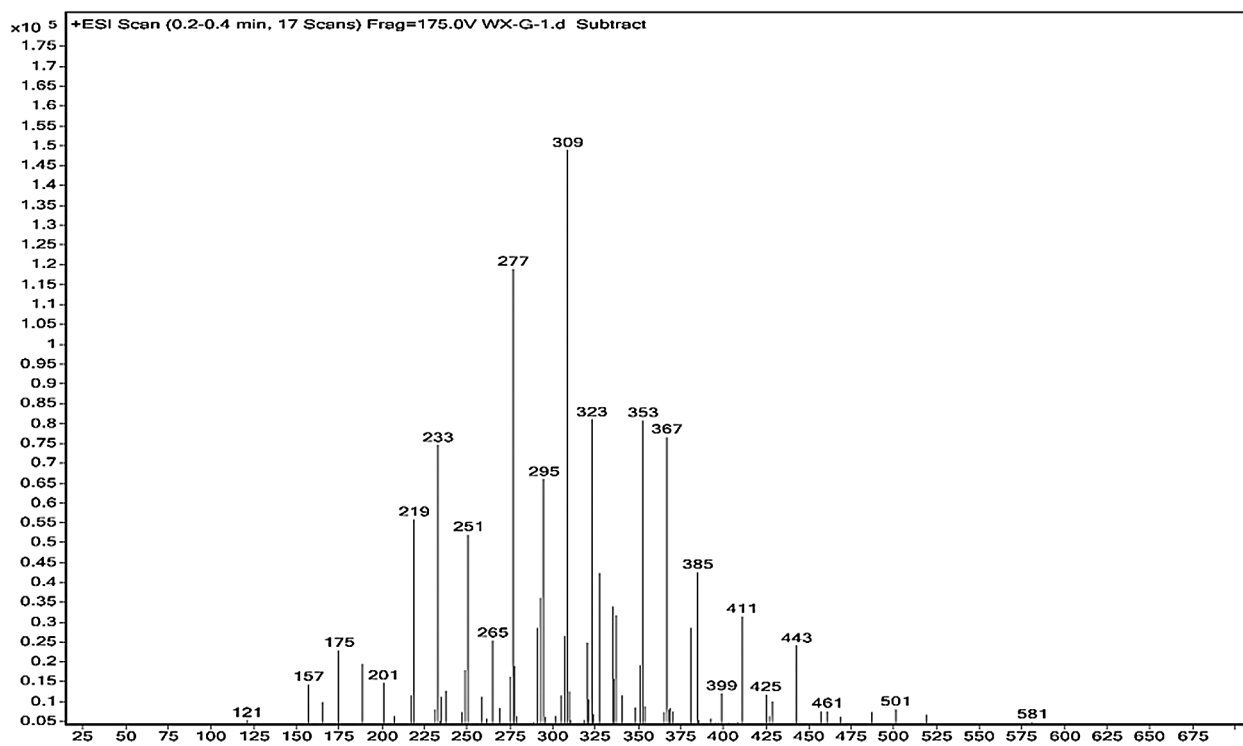


Figure 3: ESI-MS spectrum of glyoxal in acidic solution

**Table 1:** The main ion peaks of ESI-MS and their possible assignments of glyoxal in alkaline solution

Experimental (Da) [M + Na] <sup>+</sup>	Structures
121	CH <sub>2</sub> OH-COONa
219	2 CH <sub>2</sub> OH-COONa
317	3 CH <sub>2</sub> OH-COONa
415	4 CH <sub>2</sub> OH-COONa
513	5 CH <sub>2</sub> OH-COONa
611	6 CH <sub>2</sub> OH-COONa
709	7 CH <sub>2</sub> OH-COONa
807	8 CH <sub>2</sub> OH-COONa
98*n+23(n = 1,2,3...15)	n CH <sub>2</sub> OH-COONa

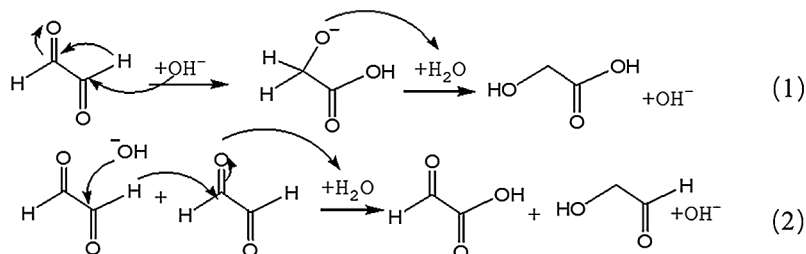
**Table 2:** The main ion peaks of ESI-MS and their possible assignments of glyoxal in acidic solution

Experimental(Da) [M + Na] <sup>+</sup>	Structures
175	
233	
251	
309	

An obvious regularity was observed from the ESI-MS spectra for the glyoxal in alkaline solution, as in Fig. 2. The molecular weight of the ion peaks at 121 Da, 219 Da, 317 Da, 415 Da, 513 Da, 611 Da, 709 Da, 807 Da, 905 Da, 1003 Da and 1101 Da showed an arithmetic progression in pattern and it had an interval of 98 Da between two adjacent ion peaks. The difference of 98 Da between two peaks could be due to CH<sub>2</sub>OH-COONa. It means that CH<sub>2</sub>OH-COOH was the main form in glyoxal solution under alkaline conditions, which came from the disproportionation reaction of one glyoxal molecule [34,35]. According to the test mechanism of ESI-MS instrument [36], the ion peaks at 219 Da, 317 Da, 415 Da, 513 Da, 611 Da, 709 Da, 807 Da, 905 Da, 1003 Da and 1101 Da came from the accumulation of CH<sub>2</sub>OH-COOH.

The possible reaction mechanism for the transformation of glyoxal under alkaline conditions is shown in Scheme 1. Both intramolecular and intermolecular disproportionation reactions in glyoxal solution are

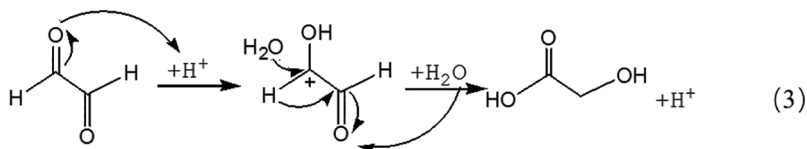
possible. Reaction 1 describes the transformation of one glyoxal molecule and Reaction 2 is the reaction between two glyoxal molecules.



**Scheme 1:** Transformations of glyoxal in alkaline solution

Both of the two reactions respect the unimolecular elimination of conjugate base (Sn1) reaction rules.  $\text{CH}_2\text{OH-COOH}$  is the main structure following the path of Reaction 1. It was also the main types of the main ion peaks observed from the ESI-MS spectra of glyoxal solution under alkaline conditions (Fig. 2 and Tab. 1). If two molecules of glyoxal reacted as Reaction 2, the ion peaks of the two resulted aldehydes with molecular weight 97 Da and 83 Da were presumed to be observed in the ESI-MS spectra of glyoxal solution. However, there were actually no obvious peaks on the two structures in Fig. 2. And the possible structure oxalic acid and glycol, gotten from the further reaction or transformation of the two resulted aldehydes were not observed, too. It indicated that glyoxal preferred to transform through an intramolecular disproportionation reaction, seen as Reaction1, to an intermolecular one under alkaline conditions. Since the process of the reduction reaction of Reaction1 would be easier than that of Reaction 2 because of the lower activity energy for the former reaction than the latter one, the ESI-MS results of glyoxal solution under alkaline conditions were theoretically reasonable.

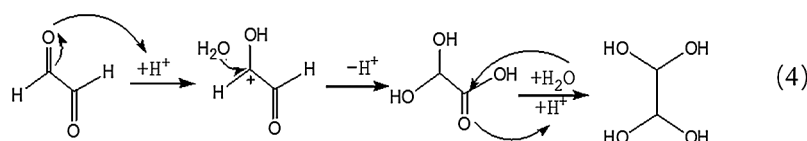
Fig. 3 is the ESI-MS result of glyoxal under acidic conditions and the assignments on their main ion peaks can be seen in Tab. 2. It seemed that the chemical formulations of glyoxal solution under acidic conditions were more complicated than those under alkaline conditions. The ion peaks at 121 Da and 219 Da, which could be assigned to  $\text{CH}_2\text{OH-COOH}$ , were detected in Fig. 3, similar to that in Fig. 2. It meant that glyoxal transformed to  $\text{CH}_2\text{OH-COOH}$  under acidic conditions as what happened under alkaline conditions. There were 18 Da difference of the molecular weight, which could be assigned as one molecule of water, between the ion peaks at 219 Da and 201 Da. The ion peak at 201 Da was then assigned to the esterification between two molecules of  $\text{CH}_2\text{OH-COOH}$ . The possible reaction mechanism for the transformation of glyoxal to  $\text{CH}_2\text{OH-COOH}$  under acid conditions is shown in Scheme 2.



**Scheme 2:** Transformations of glyoxal in acidic solution

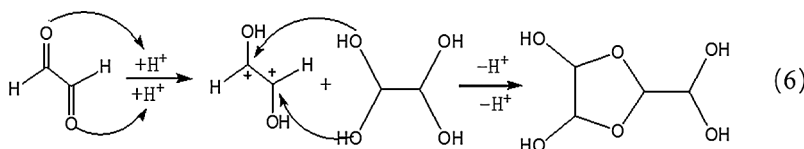
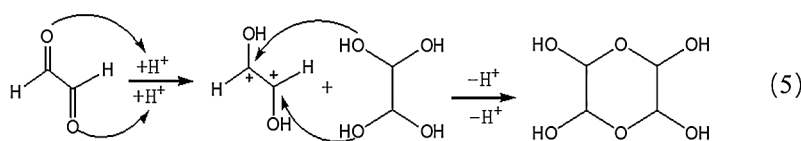
Being different from Reaction 1, for the transformation of glyoxal in acidic solution, it was  $\text{H}_2\text{O}$  rather than  $\text{OH}^-$  that attacked the carbon atom of carbonyl groups to result the disproportionation reaction, as shown in Reaction 3. Although  $\text{H}_2\text{O}$  was not a common nucleophile, the reaction between  $\text{H}_2\text{O}$  and carbonyl groups of one glyoxal molecule was possible when the electrophilicity of the carbon atom of carbonyl groups

increased, caused by the combination between the oxygen atom of the glyoxal molecule and  $H^+$  in the acidic solution. However, as shown from Fig. 3, chemical structure from the ion peaks at 121 Da and 219 Da was not the main existing forms of glyoxal in the acidic solution for their relatively lower intensity or proportion than those of other ion peaks. Since there is no  $\alpha$ -H in one molecule of glyoxal, it is presumed that it is easy for glyoxal to combine with  $H_2O$  to form ethylene tetraol under acidic conditions. The reactions to form ethylene tetraol between glyoxal and water molecules under acidic conditions are shown in Scheme 3.



**Scheme 3:** Reactions between glyoxal and water under acidic conditions

However, no obvious ion peak at around 117 Da from ethylene tetraol was detected in Fig. 3. It indicated that the resulted ethylene tetraol gotten from the combination of glyoxal and water was unstable in the acidic solution. According to the previous report on glyoxal in water [28,29], the main ion peak at 175 Da had two possible chemical structures, as seen in Tab. 2. Both of the two structures came from the etherification reaction between two molecules of ethylene tetraol. The possible reactions are shown in Scheme 4.



**Scheme 4:** Reactions between glyoxal molecules under acidic conditions

An obvious regularity was also observed from Fig. 3. The ion peak at 193 Da was the dehydrated structure of that at 175 Da. Other ion peaks at 233 Da, 251 Da and 309 Da listed in Tab. 2 were derived from the two possible structures at 175 Da.

### 3.2 $^{13}C$ -NMR Analysis of Glyoxal

$^{13}C$ -NMR was used to analyze the possible chemical structure of glyoxal solution in this study. Considering many of the possible isomers,  $^{13}C$ -NMR will give more information on the chemical structure than ESI-MS [37].

Fig. 4 is the  $^{13}C$ -NMR spectrum of glyoxal solution under alkaline conditions. Two main peaks were detected at 180.78 ppm and 62.32 ppm. They came from the absorption of carbon atom respectively of  $-COONa$  and  $-CH_2OH$  of molecule of  $CH_2OH-COOH$ . It proved that glyoxal existed in alkaline water solution mainly in form of  $CH_2OH-COOH$ . This result fitted well with that of ESI-MS. The quantity analysis indicated that  $-COOH$  and  $-CH_2OH$  had approximate content, which was in consistent with the chemical structure of  $CH_2OH-COOH$ .

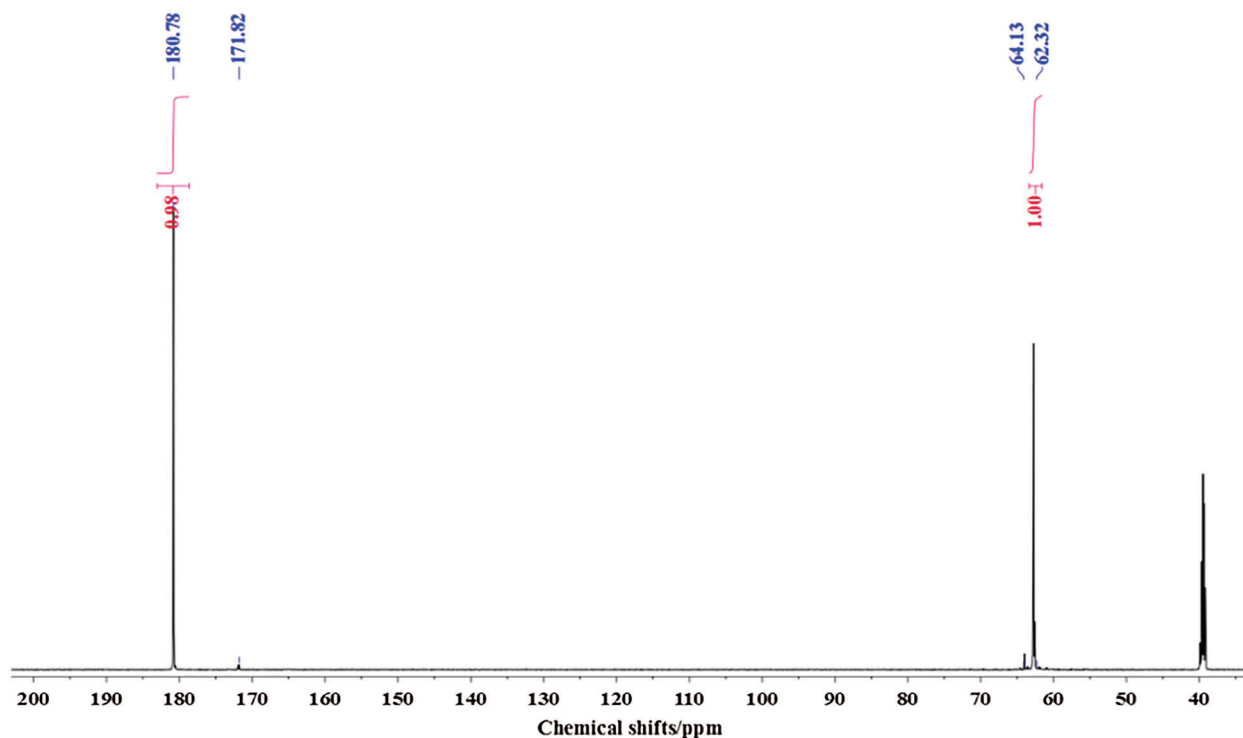


**Figure 4:**  $^{13}\text{C}$ -NMR spectrum of glyoxal in alkaline solution

Fig. 5 is the  $^{13}\text{C}$ -NMR spectrum of glyoxal solution under acidic conditions. More absorptions could be observed in Fig. 5 than Fig. 4. The peak at 63.24 and 64.15 ppm were assigned as  $\text{CH}_2\text{OHCOOH}$ . The peak at 66.30 ppm was from  $\text{HOOC-CH}_2\text{-OOC-CH}_2\text{OH}$ , gotten from the esterification between  $\text{CH}_2\text{OHCOOH}$  molecules. The peak at 167.21 ppm was from the absorption of  $\text{CH}_2\text{OHCOOH}$ . It indicated also that some of glyoxal molecules would transform to  $\text{CH}_2\text{OHCOOH}$  under acidic conditions as what had seen in ESI-MS. However, the quantity analysis of  $^{13}\text{C}$ -NMR indicated that  $\text{CH}_2\text{OHCOOH}$  was not the main form of glyoxal under acidic conditions. The main absorption appeared actually at 90–106 ppm, specifically at 90.54 ppm, 92.19 ppm, 93.59 ppm, 99.97 ppm, 100.65 ppm and 105.92 ppm. The absorption at 90–93 ppm, 95 ppm, 99–100 ppm and 105 ppm could theoretically be assigned respectively to 4 types of chemical structures with different chemical environment. According to the results of ESI-MS, all of these peaks could be assigned to the derivatives of etherate gotten from condensation reaction between two molecules of ethylene tetraol. Ethylene tetraol molecules were unstable and the etherification reaction would take place easily between these molecules [23,38] to form a ring structure. When we consider the ring tension and collision probability, five or six-membered rings showed the biggest possibility to be formed [39]. Fig. 6 summarizes the possible main etherate products units. Some of these units would unite to form other products with higher molecular weight, as shown in Fig. 3 and Tab. 2.

The possible chemical shifts of carbon atoms from different structures calculated by the software of ACD/Labs are given in Fig. 6, too [40,41]. Structure A with a five-membered ring and Structure E with a six-membered ring were the isomeric compounds. They were the main existing forms of glyoxal under acidic conditions. Structure B and Structure C were the isomeric compounds. Both of the two structures came from etherification reaction with Structure A and ethylene tetraol. Structure D was from the reaction between Structure B and ethylene tetraol. Structure F, G and H were the derivatives of Structure E.

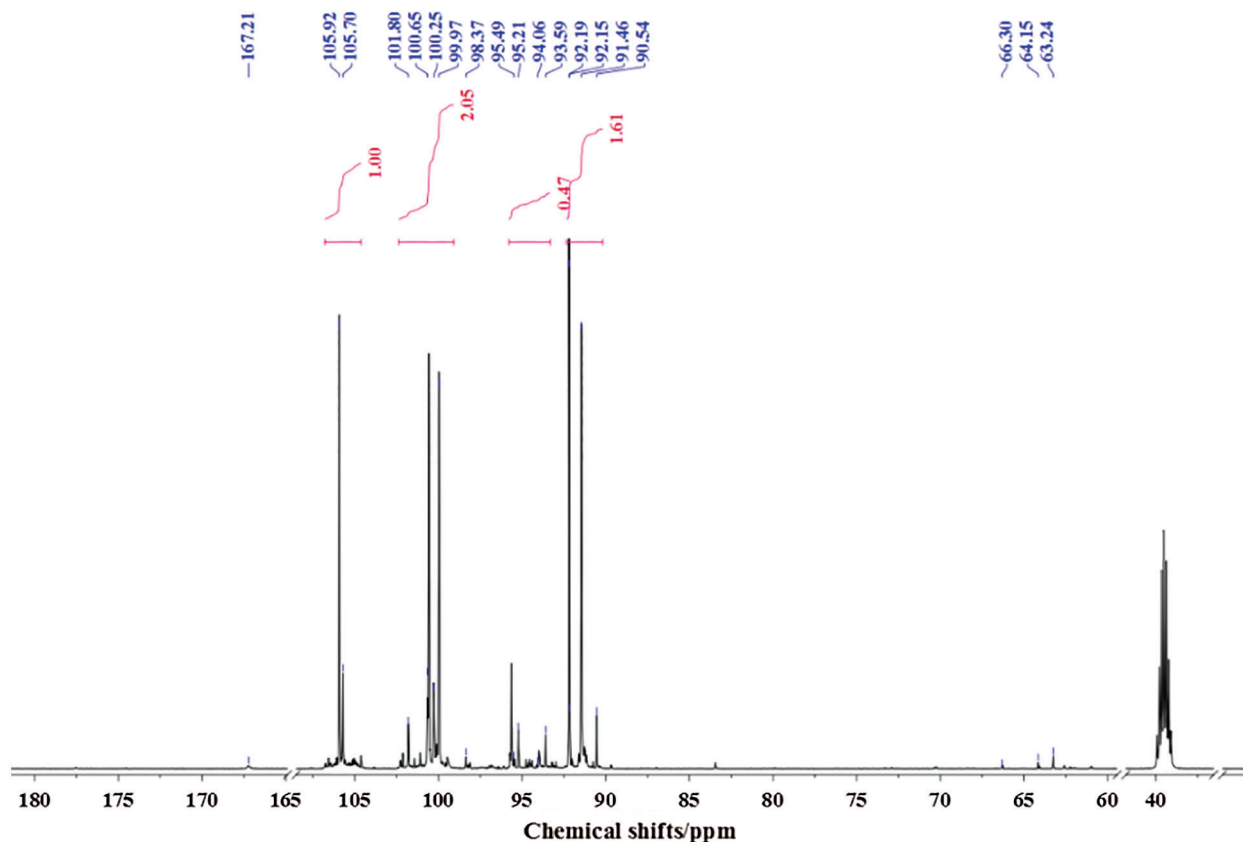


**Figure 5:**  $^{13}\text{C}$ -NMR spectrum of glyoxal in acidic solution

In Fig. 5, all of the absorptions of carbon atoms of Structure A were detected at 90–100 ppm, 105–106 ppm and 91–92 ppm. Seen from Fig. 6, only five-membered ring structure would show some absorption at 105–106 ppm. The appearance of the absorption at 105.70 ppm and 105.92 ppm proved the existence of the five-membered ring structure in the acidic solution with glyoxal.

Besides the structure of five-membered rings, the six-membered rings existed in the solution, too. If there were only structures of five-membered rings in the solution system, the molecular weight of resulted combination products would not exceed 210 Da. It was not what had been observed from its ESI-MS results. Therefore, the absorption at 91.46 ppm, 92.15 ppm, 92.19 ppm, 93.59 ppm in Fig. 5 could be assigned to both five-membered ring structure and six-membered ring structure. The absorptions at 94–95 ppm in Fig. 5 further proved the existence of six-membered ring structure in the solution with glyoxal. It might come from Structure G or Structure H. The relatively lower quantity of these absorptions indicated that the formation of Structure G or Structure H would be more difficult than Structure E and Structure F with two to three ethylene tetraol molecules. In all, glyoxal existed in forms of both five-membered ring structure and six-membered ring structure (mainly in forms of Structures A and E in Fig. 6) under acidic conditions, which were different from those forms from glyoxal under alkaline conditions. The  $^{13}\text{C}$ -NMR results on glyoxal in water at different pH levels were in consistent with the assigned structures in Tab. 2. That is to say, there is a peak in  $^{13}\text{C}$ -NMR results of Fig. 5 for every characteristic group with carbon atom of the assigned structures in ESI-MS results of Tab. 2.

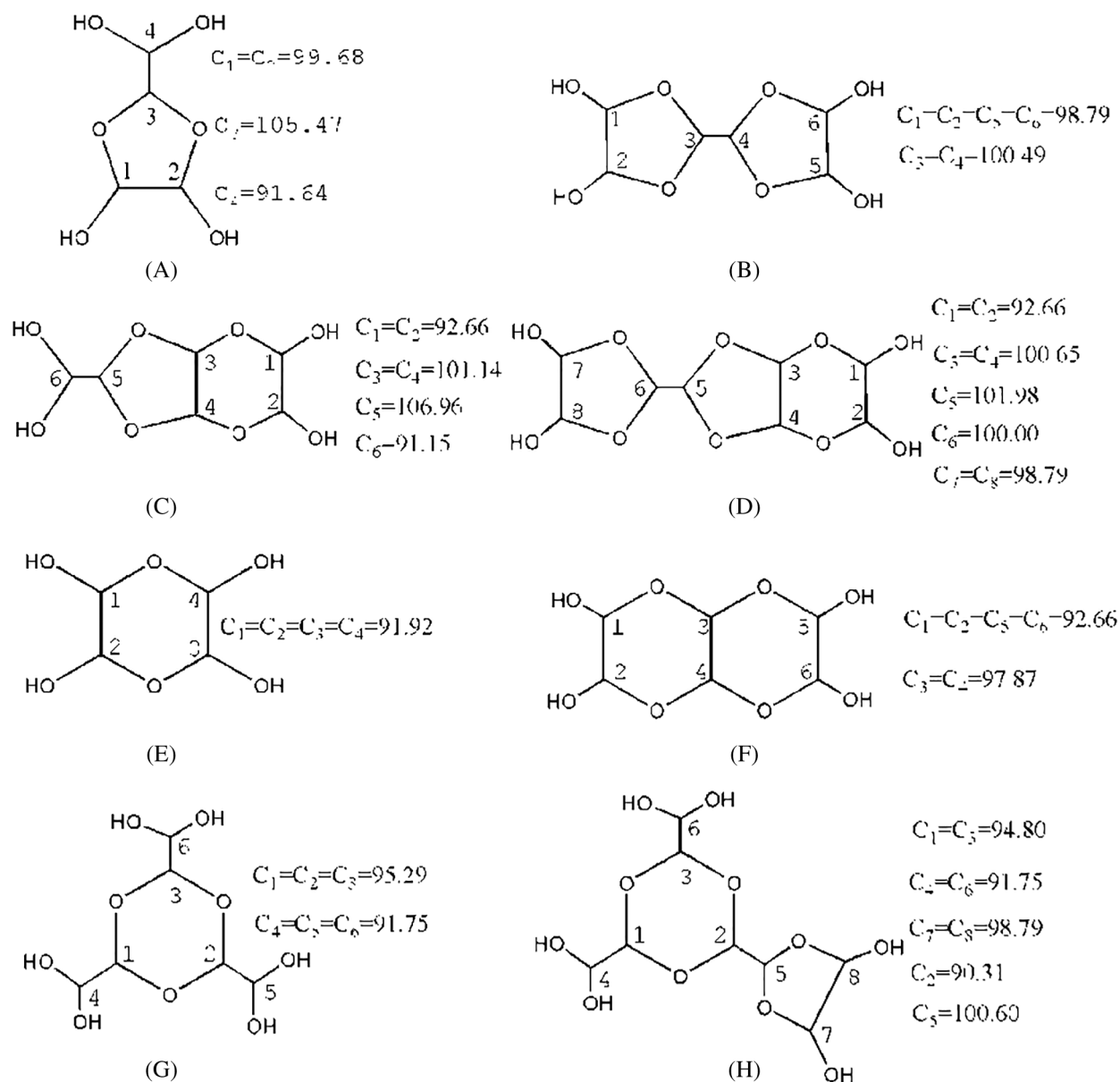


**Figure 6:** Main forms of glyoxal in acidic solution and the chemical shift calculated by software ACD/Labs

### 3.3 Performances of Soy-Based Adhesives Modified by Glyoxal Solution

The performances of soy-based adhesives modified by glyoxal solution at different pH levels are given in [Tab. 3](#). The soy-based adhesive without modification showed some dry strength but no water resistance ([Tab. 3](#)). The addition of glyoxal solution was helpful for the improvement of the water resistance of soy-based adhesives and alkaline conditions were preferable to acidic conditions for the preparation of the soy-based adhesives modified by glyoxal solution.

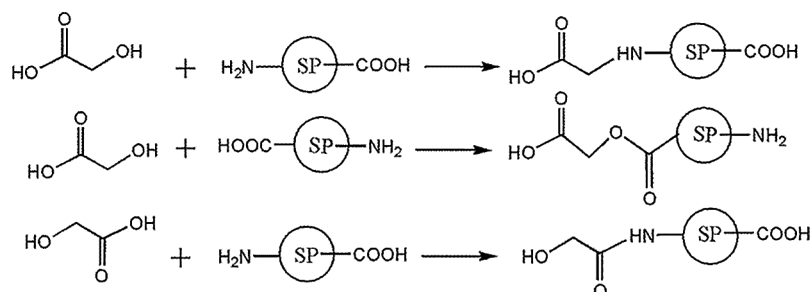
### 3.4 Mechanism of Soy-Based Adhesive Modified by Glyoxal Solution

The molecular structure of soy protein is very complex. It was too difficult to see anything whatsoever of the reaction product of soy protein and glyoxal by NMR or ESI-MS. The former results of ESI-MS and

$^{13}\text{C}$ -NMR indicated that glyoxal molecules transformed to some different derivatives in water at different pH levels. The reaction mechanism of the soy-based adhesive with glyoxal solution under alkaline or acidic conditions would then be different, too, which might be responsible to the different performances of soy-based adhesive modified by glyoxal solution. It was presumed that soy protein owned some reactive groups, such as  $-\text{NH}_2$ ,  $-\text{CONH}$ ,  $-\text{COOH}$  and  $-\text{OH}$  groups.  $\text{CH}_2\text{OHCOOH}$  was the main form of glyoxal in alkaline solution. In theory, its  $-\text{COOH}$  and  $-\text{OH}$  groups could react with soy protein. The possible reaction mechanism is shown in [Scheme 5](#).

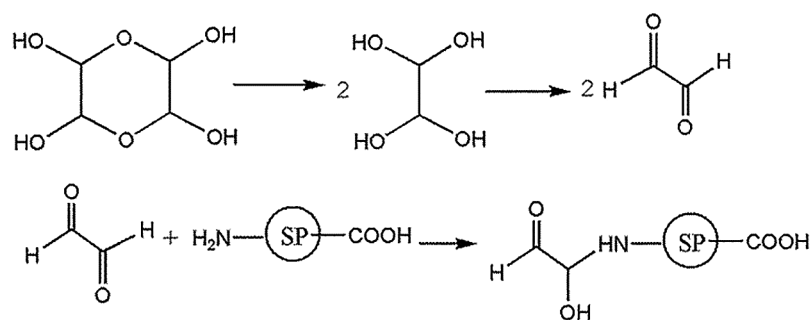
**Table 3:** Performances of soy-based adhesives modified by glyoxal solution at different pH levels

Soy-based adhesive	Dry strength/MPa	Wet strength (60°C)/MPa
SP	$0.46 \pm 0.06$	–
SPG1	$0.70 \pm 0.08$	$0.57 \pm 0.01$
SPG3	$0.94 \pm 0.09$	$0.57 \pm 0.01$
SPG11	$1.10 \pm 0.16$	$0.63 \pm 0.03$
SPG13	$1.17 \pm 0.16$	$0.85 \pm 0.01$



**Scheme 5:** Reactions between soy protein and glyoxal solution under alkaline conditions

Ethylene tetraol and their products from the etherification reaction were the main forms of glyoxal in acidic solution. The etherification reaction was reversible. The possible reaction mechanism between soy protein and glyoxal solution under acidic conditions is shown in [Scheme 6](#).



**Scheme 6:** Reactions between soy protein and glyoxal solution under acidic conditions

However, under acidic conditions, the glyoxal would react mainly with the amino groups of protein and the reaction between glyoxal and carboxyl groups of protein would be very difficult. At the same time, under

acidic conditions, the amino groups of soy protein had the tendency to combine with proton. It led the reactivity of soy protein to decrease further [42,43]. All of these led that alkaline conditions would be preferable to acidic conditions for the cross-linking of soy protein by glyoxal. This explained that why the soy protein adhesives with alkaline glyoxal solution showed better mechanical performance and water resistance than those with acidic glyoxal solution, as seen in Tab. 3.

#### 4 Conclusions

Based on the ESI-MS and  $^{13}\text{C}$ -NMR analysis on the forms of glyoxal in acidic and alkaline solutions, the soy-based adhesives cross-linked by glyoxal were prepared in this work. Some conclusions could be drawn.

1. Glyoxal existed in water in different forms at different pH levels. Under alkaline conditions, glyoxal transformed to glycolate through the intramolecular disproportionation reaction, which reduced the activity of aldehyde group of glyoxal.
2. Under acidic conditions, although some of glyoxal transformed to glycolate as what happened under alkaline conditions, most of glyoxal molecules existed in the solution in the form of five- or six-membered cyclic ether structure. The six-membered cyclic ether consisted of C,C'-p-dihydroxyl intercyclization and triethylenetetraol intercyclization. No ethylene tetraol or free aldehyde group was actually detected.
3. Although glyoxal reacted with soy protein under both acidic and alkaline conditions, alkaline conditions were more favorable for the improvement of mechanical performance and water resistance of soy-based adhesives than acid conditions, which was due to the adhesives had gotten high crosslinking density and cohesive strength.

**Funding Statement:** This work was supported by Science-technology Support Foundation of Guizhou Province of China (Nos. [2019]2325 and [2020]1Y125), the Growth Project of Young Scientific and Technological Talents in Colleges and Universities of Guizhou Province (No. [2019]184), Yunnan Fundamental Research Key Projects (No. 2019FA012), National Natural Science Foundation of China (Nos. 31870546 and 31800481).

**Conflicts of Interest:** The authors declare that they have no conflicts of interest to report regarding the present study.

#### References

1. Li, J., Luo, J., Li, X., Yi, Z., Gao, Q. et al. (2015). Soybean meal-based wood adhesive enhanced by ethylene glycol diglycidyl ether and diethylenetriamine. *Industrial Crops and Products*, 74, 613–618. DOI 10.1016/j.indcrop.2015.05.066.
2. He, G., Feng, M., Dai, C. (2013). Development of soy-based adhesives for the manufacture of wood composite products. *Holzforschung*, 66(7), 857–862. DOI 10.1515/hf-2011-0196.
3. Guo, M., Wang, G. (2016). Milk protein polymer and its application in environmentally safe adhesives. *Polymers*, 8(9), 324. DOI 10.3390/polym8090324.
4. Shi, J., Wen, M., Li, X., Xu, W., Li, Z. (2018). Research progress of biomass-based formaldehyde-free adhesives. *Journal of Forestry Engineering*, 3(2), 1–10. DOI 10.13360/j.issn.2096.
5. Gao, Q., Liu, Z., Li, J. (2020). Research progress of soy protein adhesive for wood-based composites. *Journal of Forestry Engineering*, 5(2), 1–11. DOI 10.13360/j.issn.2096.
6. Damodaran, S., Zhu, D. (2016). A formaldehyde-free water-resistant soy flour-based adhesive for plywood. *Journal of the American Oil Chemists' Society*, 93(9), 1311–1318. DOI 10.1007/s11746-016-2866-x.
7. Sang, Z., Zhang, S., Gao, Q., Li, J. (2010). Preparation and application of modified soybean protein adhesives. *Advanced Materials Research*, 139–141, 706–709. DOI 10.4028/www.scientific.net/AMR.139-141.706.

8. Ji, N., Long, J., Zheng, H., He, J. (2011). Phenolic resin modified soybean protein adhesive. *Advanced Materials Research*, 236–238, 3–7. DOI 10.4028/www.scientific.net/AMR.236-238.3.
9. O'Dell, J. L., Hunt, C. G., Frihart, C. R. (2013). High temperature performance of soy-based adhesives. *Journal of Adhesion Science and Technology*, 27(18–19), 2027–2042. DOI 10.1080/01694243.2012.69694.
10. Qu, P., Huang, H., Wu, G., Sun, E., Chang, Z. (2015). The effect of hydrolyzed soy protein isolate on the structure and biodegradability of urea-formaldehyde adhesives. *Journal of Adhesion Science and Technology*, 29(6), 502–517. DOI 10.1080/01694243.2014.995909.
11. Qu, P., Huang, H., Wu, G., Sun, E., Chang, Z. (2015). Hydrolyzed soy protein isolates modified urea-formaldehyde resins as adhesives and its biodegradability. *Journal of Adhesion Science and Technology*, 29(21), 2381–2398. DOI 10.1080/01694243.2015.1067176.
12. Qi, G., Sun, X. S. (2011). Soy protein adhesive blends with synthetic latex on wood veneer. *Journal of the American Oil Chemists' Society*, 88(2), 271–281. DOI 10.1007/s11746-010-1666-y.
13. Gao, Q., Shi, S. Q., Zhang, S., Li, J., Wang, X. et al. (2012). Soybean meal-based adhesive enhanced by MUF resin. *Journal of Applied Polymer Science*, 125(5), 3676–3681. DOI 10.1002/app.36700.
14. Fan, D., Qin, T., Chu, F. (2011). A soy flour-based adhesive reinforced by low addition of MUF resin. *Journal of Adhesion Science and Technology*, 25(1–3), 323–333. DOI 10.1163/016942410X524147.
15. Lei, H., Du, G., Wu, Z., Xi, X., Dong, Z. (2014). Cross-linked soy-based wood adhesives for plywood. *International Journal of Adhesion and Adhesives*, 50, 199–203. DOI 10.1016/j.ijadhadh.2014.01.026.
16. Deng, S., Pizzi, A., Du, G., Zhang, J., Zhang, J. (2014). Synthesis, structure, and characterization of glyoxal-urea-formaldehyde co-condensed resins. *Journal of Applied Polymer Science*, 131(21), 41009–41018. DOI 10.1002/app.41009.
17. Deng, S., Du, G., Li, X., Pizzi, A. (2014). Performance and reaction mechanism of zero formaldehyde-emission urea-glyoxal (UG) resin. *Journal of the Taiwan Institute of Chemical Engineers*, 45(4), 2029–2038. DOI 10.1016/j.jtice.2014.02.007.
18. Wu, Z., Lei, H., Cao, M., Xi, X., Liang, J. et al. (2016). Soy-based adhesive cross-linked by melamine-glyoxal and epoxy resin. *Journal of Adhesion Science and Technology*, 30(19), 2120–2129. DOI 10.1080/01694243.2016.1175247.
19. Ballerini, A., Despres, A., Pizzi, A. (2005). Non-toxic, zero emission tannin-glyoxal adhesives for wood panels. *Holz Als Roh- Und Werkstoff*, 63(6), 477–478. DOI 10.1007/s00107-005-0048-x.
20. Wang, X., Wu, Z., Lei, H., Wu, J., Su, L. et al. (2017). Tannin-based adhesive prepared by glyoxal. *Chinese Journal of Adhesion*, 26(2), 39–42. DOI 10.13416/j.ca.2017.02.010.
21. Lei, H., Pizzi, A., Du, G. (2008). Environmentally friendly mixed tannin/lignin wood resins. *Journal of Applied Polymer Science*, 107(1), 203–209. DOI 10.1002/app.27011.
22. El Mansouri, N., Pizzi, A., Salvadó, J. (2007). Lignin-based wood panel adhesives without formaldehyde. *Holz Als Roh- Und Werkstoff*, 65(1), 65–70.
23. Amaral-Labat, G. A., Pizzi, A., Gonçalves, A. R., Celzard, A., Rigolet, S. et al. (2008). Environment-friendly soy flour-based resins without formaldehyde. *Journal of Applied Polymer Science*, 108(1), 624–632. DOI 10.1002/app.27692.
24. Wu, Z., Xi, X., Lei, H., Liang, J., Liao, J. et al. (2019). Study on soy-based adhesives enhanced by phenol formaldehyde cross-linker. *Polymers*, 11(2), 365. DOI 10.3390/polym11020365.
25. Younesi-Kordkheili, H., Pizzi, A. (2016). Acid ionic liquids as a new hardener in urea-glyoxal adhesive resins. *Polymers*, 8(3), 57. DOI 10.3390/polym8030057.
26. Vaz, C. M., van Doeveren, P. F. N. M., Yilmaz, G., de Graaf, L. A., Reis, R. L. et al. (2005). Processing and characterization of biodegradable soy plastics: Effects of crosslinking with glyoxal and thermal treatment. *Journal of Applied Polymer Science*, 97(2), 604–610. DOI 10.1002/app.20609.
27. Xu, P., Wu, C., Fan, G., Zhang, C., Gao, X. et al. (2019). Preparation and characteristic evaluation of *Lactobacillus plantarum* microcapsules developed with the ginkgo seed protein and sodium alginate. *Journal of Forestry Engineering*, 4(5), 70–77. DOI 10.13360/j.issn.2096.

28. Whipple, E. B. (1970). Structure of glyoxal in water. *Journal of the American Chemical Society*, *92*(24), 7183–7186. DOI 10.1021/ja00727a027.
29. Bedford, C. T., Fallah, A., Mentzer, E., Williamson, F. A. (1992). The first characterization of a glyoxal-hydrogen sulfide adduct. *Journal of the Chemical Society, Chemical Communications*, *15*(15), 1035–1036. DOI 10.1039/C39920001035.
30. Kliegman, J. M., Whipple, E. B., Ruta, M., Barnes, R. K. (1972). Glyoxal derivatives. IV. 2-Dimethoxymethyl-4,5-dimethoxy-1,3-dioxolane and 2,2'-bis(4,5-dimethoxy-1,3-dioxolane). *Journal of Organic Chemistry*, *37*(8), 1276–1279. DOI 10.1021/jo00973a051.
31. Gallezot, P. (1992). Catalytic oxidation of glyoxal to glyoxylic acid on platinum metals. *Journal of Catalysis*, *133*(2), 479–485. DOI 10.1016/0021-9517(92)90255-G.
32. Liang, J., Wu, Z., Lei, H., Xi, X., Li, T. et al. (2017). The reaction between furfuryl alcohol and model compound of protein. *Polymers*, *9*(12), 711. DOI 10.3390/polym9120711.
33. Liang, J., Wu, Z., Xi, X., Lei, H., Zhang, B. et al. (2019). Investigation of the reaction between a soy-based protein model compound and formaldehyde. *Wood Science and Technology*, *53*(5), 1061–1077. DOI 10.1007/s00226-019-01118-8.
34. Nguyen, H. P., Schug, K. A. (2008). The advantages of ESI-MS detection in conjunction with HILIC mode separations: Fundamentals and applications. *Journal of Separation Science*, *31*(9), 1465–1480. DOI 10.1002/jssc.200700630.
35. Fratzke, A. R., Reilly, P. J. (1986). Kinetic analysis of the disproportionation of aqueous glyoxal. *International Journal of Chemical Kinetics*, *18*(7), 757–773. DOI 10.1002/kin.550180704.
36. Loeffler, K. W., Koehler, C. A., Paul, N. M., De Haan, D. O. (2006). Oligomer formation in evaporating aqueous glyoxal and methyl glyoxal solutions. *Environmental Science & Technology*, *40*(20), 6318–6323. DOI 10.1021/es060810w.
37. Nicholson, J. K., Foxall, P. J. D., Spraul, M. (1995). 750 MHz  $^1\text{H}$  and  $^1\text{H}$ - $^{13}\text{C}$  NMR spectroscopy of human blood plasma. *Analytical Chemistry*, *67*(5), 793–811. DOI 10.1021/ac00101a004.
38. Veyret, B., Roussel, P., Lesclaux, R. (1984). Absolute rate constant for the disproportionation reaction of formyl radicals from 295 to 475 K. *Chemical Physics Letters*, *103*(5), 389–392. DOI 10.1016/0009-2614(84)80326-7.
39. Petechuk, V. M. (2010). Stability of rings. arXiv preprint arXiv: 1003.2301.
40. Martin, G. E., Hadden, C. E., Russell, D. J., Kaluzny, B. D., Guido, J. E. et al. (2002). Identification of degradants of a complex alkaloid using NMR cryoprobe technology and ACD/structure elucidator. *Journal of Heterocyclic Chemistry*, *39*(6), 1241–1250. DOI 10.1002/jhet.5570390619.
41. Fereyduni, E., Rofouei, M. K., Kamaee, M., Ramalingam, S., Sharifkhani, S. M. (2012). Single crystal structure, spectroscopic (FT-IR, FT-Raman,  $^1\text{H}$  NMR,  $^{13}\text{C}$  NMR) studies, physico-chemical properties and theoretical calculations of 1-(4-chlorophenyl)-3-(4-nitrophenyl) triazene. *Spectrochimica Acta Part A: Molecular and Biomolecular Spectroscopy*, *90*, 193–201. DOI 10.1016/j.saa.2012.01.032.
42. Zhang, L., Xu, M., Hu, X., Wang, Y. (2017). Study on binding of EGCG-Cu complex to bovine serum albumin. *Journal of Forestry Engineering*, *2*(5), 46–50. DOI 10.13360/j.issn.2096.
43. Lei, H., Wu, Z., Cao, M., Du, G. (2016). Study on the soy protein-based wood adhesive modified by hydroxymethyl phenol. *Polymers*, *8*(7), 256. DOI 10.3390/polym8070256.